



# Metabolically Active Microbial Communities in Acidic Uranium-Contaminated Subsurface Sediments

Heath J. Mills, Denise M. Akob, Lainie Petrie-Edwards, Thomas M. Gihring, Joel E. Kostka  
Department of Oceanography, Florida State University, Tallahassee, FL



Health J. Mills  
326 Nuclear Research Building  
Florida State University  
Tallahassee, FL 32312  
mills@ocean.fsu.edu

## ABSTRACT

Uranium contamination is widespread in subsurface sediments at nuclear weapons production sites in the United States and Eastern Europe. Due to the uranium extraction process, waste disposal practices and varying groundwater flow patterns, sediments range from neutral to acidic pH and are co-contaminated with variable concentrations of nitrate. Current bioremediation strategies attempt to stimulate indigenous metal-reducing microbial communities through substrate addition to effectively immobilize uranium in the contaminated subsurface. However, the diversity of active microbial groups prior to and after substrate addition is currently unknown. The objective of this study was to characterize the metabolically-active fraction of the in situ microbial community across vertical depth and geochemical gradients to provide an initial point of reference for determination of the impacts of bioremediation practices on functional diversity. A cultivation-independent approach targeting SSU rRNA sequences was used to compare the *in situ* microbial communities within acidic (pH 3-4) and near neutral pH (pH 6-7) zones of contaminated subsurface sediments collected from a single bore hole (FB61) at the US DOE Field Research Center (FRC), Oak Ridge, TN. Samples were collected from four sediment depths (2.1 - 4.6 m below surface), where a large gradient in nitrate concentration was observed along with sediment pH. A total of 8 clone libraries were constructed from amplified bacterial SSU rRNA genes (DNA-derived) and cDNA reverse transcribed from SSU rRNA (RNA-derived). Clones were screened using restriction fragment length polymorphism analysis, followed by sequencing of cloned inserts. Clone restriction was most related to the phyla *Firmicutes*, *Proteobacteria*, *Actinobacteria*, and *Planctomycetes*. The diversity and numerical dominance of phylotypes varied between the DNA- and RNA-derived libraries. The most abundant phylotypes found in the DNA-derived libraries were members of the class *Alphaproteobacteria*, while sequences related to the class *Gammaproteobacteria* were more frequently detected in the RNA-derived libraries. Each library was statistically unique, however libraries constructed from similar pH sediments were the most similar, suggesting pH has a higher selective pressure on the active and total microbial community than other geochemical parameters studied (uranium, iron, or nitrate). Through identification of the metabolically-active members of microbial communities, our results point to microbial groups which may have a higher bioremediation potential in the uranium-contaminated subsurface. Our improved approach and extensive sequence database further provide the foundation for determination of the response of metal-reducers and other heterotrophic groups to biostimulation in the field and in sediment microcosms.

## BACKGROUND

The U.S. Department of Energy (DOE) has established the Natural and Accelerated Bioremediation Research (NABIR) Program in order to develop cost-effective bioremediation strategies for the decontamination of metal-radionuclide wastes. NABIR has conducted field bioremediation studies at the Field Research Center (FRC) located at the Y-12 complex near the Oak Ridge National Laboratory, Oak Ridge, TN (Figure 1A). Similar to many other DOE sites across the U.S., the FRC site is co-contaminated with [U(VI)] and nitric acid. [U(VI)] is highly soluble in groundwater but can be reduced by both chemical and biological processes to an insoluble state, i.e., [U(IV)].

Current bioremediation strategies are focused on stimulating metal-reducing microbial communities which can mediate the reduction of [U(VI)] to [U(IV)]. Such communities have been stimulated by carbon substrate addition and pH neutralization in both *in situ* and microcosm studies (Petrie et al. 2003; North et al. 2004). Because nitrate is a competing electron acceptor for metal-reducing bacteria, nitrate must be depleted prior to the onset of metal reduction (Fineran et al. 2002; Senko et al. 2002). The bioremediation potential of a selected site is subject to the diversity and metabolic state of microorganisms capable of catalyzing contaminant immobilization. These microorganisms respond to both geochemical concentrations and ecological interactions between microbial populations. Thus, an understanding of the structure and functional relationships of microbial communities across geochemical gradients is critical for the design of successful metal-radionuclide bioremediation strategies.

FIGURE 1: Map showing the location of the NABIR Field Research Center (FRC) at Oak Ridge National Laboratory, Oak Ridge, TN (A) and the location of the Area 1 study site (B). Sediment cores used in this study were extracted from bore hole FB61 (C).



## SPECIFIC GOALS

- Characterize the microbial community within Area 1 borehole FB61 using cloning and sequencing techniques targeting the SSU rRNA.
- Determine variations in microbial community structure (i.e. diversity and phylogenetic composition) with depth and across geochemical gradients within borehole FB61.
- Compare the total bacterial community (SSU rRNA gene-derived) to the metabolically-active fraction (SSU rRNA-derived) within acidic and neutral pH sediments of borehole FB61.

## METHODS

- Sediment samples were collected from the Area 1 experimental plot at the Field Research Center (FRC) (Figure 1B).
- A GeoProbe was used to sample subsurface sediments of borehole FB61 and sub-sampled under anoxic conditions.
- Sub-samples from each depth interval were frozen at -80°C until nucleic acid extraction.
- Samples were chosen for molecular analysis based on their geochemical characteristics (Table 1).
- Total nucleic acids were extracted from sediments using the method of Hurl et al. 2001.
- Clone libraries were constructed from PCR amplified 16S rRNA products.
- Clones were screened using restriction fragment length polymorphism analysis (RFLP) and unique clones were sequenced.
- Representative clones from the resulting phylotypes were sequenced for phylogenetic analysis.

TABLE 1: Sediment characteristics of contaminated Area 1 borehole FB61.

Depth Interval	Depth (m)	pH	Nitrate <sup>1</sup>	Fe-oxalate extract <sup>2</sup>	Nitrate reduction rates <sup>3</sup>	Fe(II) production rates <sup>2</sup>
61-01-00	2.4-3.1	6.7	0.6	31.5	0.70 ± 2.84	0.00 ± 1.44
61-01-24	3.1-3.7	6.1	0.1	17.0	0.70 ± 3.30	0.01 ± 0.25
61-03-00	4.9-5.5	3.9	17.8	17.3	0.70 ± 1.30	ND <sup>3</sup>
61-03-25	5.5-6.1	3.7	40.1	18.6	0.01 ± 2.84	0.00 ± 0.82

<sup>1</sup>Units in μmol g<sup>-1</sup>. <sup>2</sup>Units in μmol g<sup>-1</sup> d<sup>-1</sup>, data reported in Petrie et al. in review. <sup>3</sup>Not determined.

TABLE 2: Diversity and distribution of SSU rRNA gene clones (DNA-derived) from borehole FB61.

Phylogenetic Group	Clone Designation	Sequence Related	Number of related clones in each depth			
			61-01-00	61-01-24	61-03-00	61-03-25
Firmicutes	61-01-24001	<i>Methylobacterium</i> sp. strain SCS 19	99	0	0	0
	61-01-24008	<i>Sphingomonas acidophilicarpa</i>	97	8	2	0
	61-01-24012	<i>Sphingomonas acidophilicarpa</i>	98	6	3	0
	61-01-24015	Soil clone W2027	95	5	2	0
	61-01-24019	<i>Sphingomonas acidophilicarpa</i>	98	1	2	0
	61-01-24020	<i>Sphingomonas</i> sp. 4440	98	2	2	0
	61-01-24021	<i>Cellulomonas</i> sp. 4440	99	2	2	0
	61-01-24023	<i>Bradyrhizobium</i> sp. Phs-8	93	1	0	1
	61-01-24081	<i>Cellulomonas</i> sp. strain FW28	99	2	2	0
	61-01-24090	<i>Rhizobium</i> sp. K4	98	1	0	0
Actinobacteria	61-01-06012	<i>Sphingomonas</i> sp. C22	99	1	1	0
	61-01-23111	<i>Actinomyces</i> sp. IM1-37878	97	29	4	0
	61-01-23243	Soil clone CFC7-C	94	24	0	21
	61-01-24097	<i>Caulobacter</i> clone 6142544b48	99	7	4	0
	61-01-25202	<i>Actinomyces</i> sp. TDEB1	98	4	0	3
	61-01-06006	<i>Actinomyces</i> sp. TDEB1	99	3	0	0
	61-01-06013	Oxygen transferer biofilm clone L11	99	1	0	1
	61-01-25195	Oxygen transferer biofilm clone L11	96	1	0	1
	61-01-25119	<i>Actinomyces</i> sp. KSP2	96	1	0	1
	61-01-25136	NABIR FRC clone MRC-011	99	1	0	1
Proteobacteria	61-01-06047	<i>Actinomyces</i> sp. 98-43833	94	1	0	1
	61-01-06027	<i>Actinomyces</i> sp. 98-43833	99	1	0	0
	61-01-06021	<i>Actinomyces</i> sp. 98-43833	99	1	0	0
	61-01-24001	Deep-sea sediment clone B66-5	99	24	0	24
	61-01-24002	<i>Actinomyces</i> sp. strain LH3313	98	23	11	0
	61-01-24009	<i>Actinomyces</i> sp. strain LH3313	99	20	1	0
	61-01-24016	<i>Termonaphys</i> sp. strain LH3313	99	4	1	0
	61-01-24017	<i>Actinomyces</i> sp. 11	99	4	1	0
	61-01-04009	Clone BL011B19	99	1	1	0
	61-01-04079	<i>Neurospora</i> sp. C157	97	1	1	0
Bacteroidetes	61-01-06043	Biomass-reducing bacterium B7	98	1	0	0
	61-01-06042	<i>Neurospora</i> sp. C157	97	1	1	0
	61-01-06045	<i>Mycobacterium</i> sp. Subak-2	97	1	1	0
	61-01-06049	Clone CH1-1_BAC168RNA-9N-EP8	99	49	2	0
	61-01-06052	Type 160 strain F80C	98	3	0	13
	61-01-23112	Biofilm clone MTA19	96	2	0	2
	61-01-24019	Clone CH1-1_BAC168RNA-9N-EP8	99	1	0	17
	61-01-24014	Isolate 4-1780	99	1	1	0
	61-01-06051	<i>Streptomyces</i> sp. strain 209	99	12	0	0
	61-01-06056	<i>Streptomyces</i> sp. strain CVS	99	7	0	7
Firmicutes	61-01-06017	<i>Streptomyces</i> sp. strain ATCC 10556	99	1	0	0
	61-01-24032	<i>Rhizoglyphus</i> clone w0198	99	2	1	0
	61-01-24019	Clone NAB32	99	1	0	0

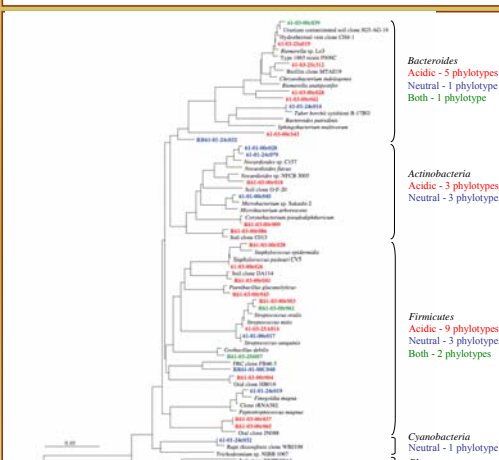


FIGURE 2: Phylogenetic tree of non-Proteobacteria-related clone sequences from FB61 sediment samples and selected related cultured isolates and environmental clones. Phylotypes specific to acidic pH sediment are red, neutral pH sediments are blue, and both are green. RNA-derived clones begin with "R" or "RR".

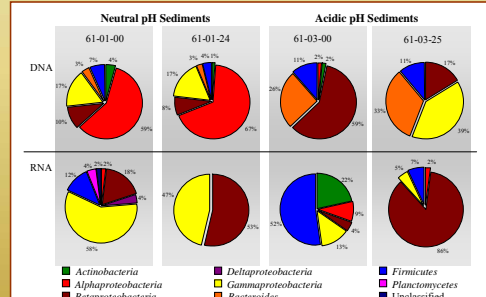


FIGURE 3: Diversity and distribution of SSU rRNA clones (RNA-derived) from borehole FB61.

TABLE 3: Diversity and distribution of SSU rRNA clones (RNA-derived) from borehole FB61.

Phylogenetic Group	Clone Designation	Sequence Related	% Similarity			
			61-01-00	61-01-24	61-03-00	61-03-25
Firmicutes	R61-01-00308	<i>Sphingomonas</i> sp. C22	99	1	0	0
	R61-01-00310	Waters biofilm clone D	99	2	0	1
	R61-01-00314	Biofilm larval clone D	99	1	0	0
	R61-01-00401	<i>Actinomyces</i> sp. Hs-11	99	16	2	14
	R61-01-24013	<i>Actinomyces</i> sp. Hs-11	99	5	0	5
	R61-01-24011	<i>Actinomyces</i> sp. Hs-11	99	1	0	0
	R61-01-24042	<i>Actinomyces</i> sp. Hs-11	99	3	0	3
	R61-01-00357	<i>Radiobacter</i> sp. 13A	99	41	2	36
	R61-01-25112	<i>Bacteroides</i> sp. parvulus	97	1	0	0
	R61-01-00352	<i>Neurospora</i> -contaminated soil clone 27	99	1	0	0
Proteobacteria	R61-01-00393	<i>Neurospora</i> -contaminated soil clone 27	99	1	0	0
	R61-01-00356	<i>Radiobacter</i> sp. Q3-011A	99	1	0	1
	R61-01-00319	Soil clone PA012	97	2	2	0
	R61-01-00329	<i>Rhizobium</i> sp. BPC	99	19	7	9
	R61-01-00321	<i>Rhizobium</i> sp. BPC	99	2	2	0
	R61-01-00325	<i>Rhizobium</i> sp. BPC	99	1	0	1
	R61-01-24032	Sediment clone S-N025-25A	98	1	0	1
	R61-01-00318	Soil clone PE (G11) A-2	100	1	0	1
	R61-01-00318	<i>Neurospora</i> sp. NCFB 3005	100	1	0	1
	R61-01-00356	Soil clone Q4-20	99	1	0	1
Actinobacteria	R61-01-00389	<i>Coriobacterium</i> sp. strain Y11	99	3	0	3
	R61-01-00357	<i>Cellulomonas</i> sp. strain TTT	99	8	2	2
	R61-01-00317	Soil clone N088	99	2	0	2
	R61-01-00383	<i>Streptomyces</i> sp. strain SwPI	99	2	0	1
	R61-01-00384	Soil clone T880A	99	1	0	1
	R61-01-00328	<i>Streptomyces</i> sp. strain epidermis	100	1	0	1
	R61-01-00341	Soil clone H14	99	1	0	1
	R61-01-00343	<i>Planctomyces</i> sp. strain ATCC 30623	98	1	0	1
	R61-01-00361	<i>Streptomyces</i> sp. strain ATCC 30623	99	2	0	2
	R61-01-00365	Soil clone N088	99	2	0	2
Planctomycetes	R61-01-00368	Soil clone T9085A-14	96	2	2	2
	R61-01-00368	Forest soil clone F18 F18	95	1	0	0

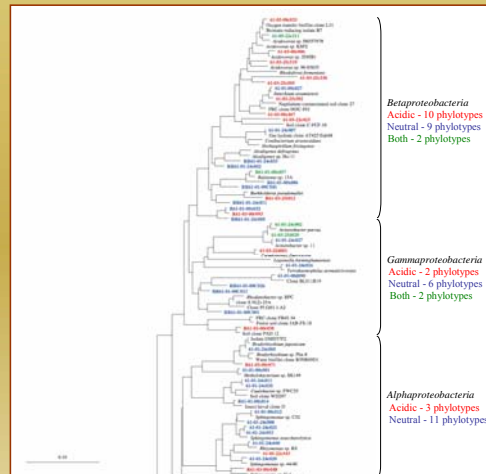


FIGURE 3: Phylogenetic tree of Proteobacteria-related clone sequences from FB61 sediment samples and selected related cultured isolates and environmental clones. Phylotypes specific to acidic pH sediment are red, neutral pH sediments are blue, and both are green. RNA-derived clones begin with "R" or "RR".

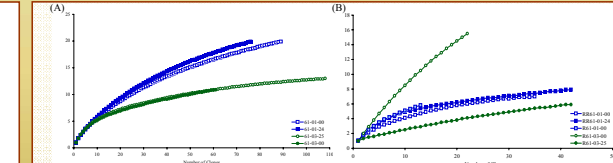


FIGURE 4: Rarefaction curves for the number of unique OTUs versus the number of clones sampled from (A) DNA-derived and (B) RNA-derived clone libraries. OTUs were defined as different RFLP patterns resulting from digestion of clones with the restriction endonucleases HaeIII and MspI.

TABLE 4: Characteristics and diversity estimates for SSU rRNA clones from FB61 sediment samples.

Target	Primer Set	Samples	No. of Clones	OTUs <sup>1</sup>	Species Richness	Shannon-Wiener <sup>2</sup>	1/D <sup>3</sup>	Percent Coverage <sup>4</sup>	H <sub>sp</sub> <sup>5</sup>	Nucleotide Diversity <sup>6</sup>	Gene Diversity <sup>7</sup>
DNA	27F/1392R	61-01-00	90	20	29 (22, 56) <sup>8</sup>	2.09	4.22	90.0	172.8 ± 82.7 <sup>9</sup>	0.15 ± 0.07	0.76 ± 0.04
		61-01-24	77	20	27 (22, 49)	2.19	4.72	88.3	167.8 ± 80.3	0.14 ± 0.07	0.79 ± 0.05
		61-03-00	62	11	21 (13, 63)	1.86	5.25	91.9	172.3 ± 82.9	0.15 ± 0.07	0.81 ± 0.03
		61-03-25	109	13	14 (13, 21)	1.98	5.78	97.3	204.3 ± 97.6	0.18 ± 0.08	0.83 ± 0.02
RNA	1055F/1392R	R61-01-00	36	7	7 (7, 7)	1.39	2.93	97.2	22.78 ± 11.32	0.06 ± 0.03	0.73 ± 0.04
		R61-01-24	43	8	11 (8, 33)	1.72	5.33	93.0	21.69 ± 10.83	0.06 ± 0.03	0.81 ± 0.03
		R61-01-00	14	6	8 (6, 21)	1.57	5.55	78.6	68.32 ± 35.22	0.16 ± 0.08	0.81 ± 0.07
		R61-03-00	23	16	30 (20, 63)	2.67	28.11	52.2	88.36 ± 43.99	0.19 ± 0.09	0.86 ± 0.02
		R61-03-25	43	6	7 (6, 16)	0.7	1.43	93.0	32.12 ± 15.87	0.21 ± 0.13	0.90 ± 0.09

<sup>1</sup>Operational taxonomic units based on RFLP analysis. <sup>2</sup>Shannon-Wiener Index, higher number represents higher diversity. <sup>3</sup>Shannon's Reciprocal Index, higher number represents higher diversity. <sup>4</sup>Percent Coverage, calculated from the following C = 1/(1/N)<sup>100</sup> \* 100, average species divergence calculated from the number of nucleotide differences between two random sequence from a population. <sup>5</sup>Nucleotide diversity, higher number indicates higher divergence of sequences. <sup>6</sup>Gene diversity, higher number indicates higher divergence of sequences. The numbers in parenthesis are 95% confidence intervals. <sup>7</sup>Mean ± standard deviation.

FIGURE 5: Representative microbial community diversity patterns and evenness based on OTU abundance in depth intervals of borehole FB61. Evenness is presented in boxes, as the value approaches 1 the population is more evenly distributed.

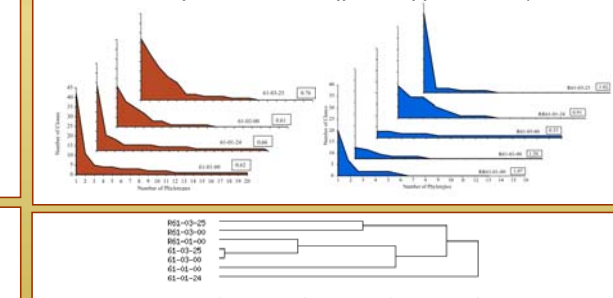


FIGURE 5: Dendrogram of LIBSHUFF comparative analysis of sequences from DNA-derived and RNA-derived clone libraries for each depth interval of FB61. The dendrogram was calculated from a matrix of 6C<sub>xy</sub> values with the lowest p-value. The x-axis is a correlation measure based on distance between 6C<sub>xy</sub>.

## CONCLUSIONS

- Differences in taxa distribution and diversity at the phylotype level were observed between DNA- and RNA-derived clone libraries from acidic and neutral pH sediment and across various environmental parameters, such as nitrate and iron concentrations. Statistical analysis indicated slightly higher diversity in neutral sediment clone libraries compared to acidic pH sediments libraries. RNA-derived clone libraries contained fewer taxa compared to the DNA-derived clone libraries. Interestingly, the taxa distribution, numerically dominated by *Firmicutes*, *Beta-* and *Gammaproteobacteria*, was similar to the acidic pH derived DNA clone libraries.
- Numerous phylotypes had high sequence similarity to cultured organisms capable of nitrate reduction and clones from other FRC studies of groundwater and sediments microbial communities (Yan et al. 2003; North et al. 2004; Palumbo et al. 2004; Reardon et al. 2004; Fields et al. 2005). These results together with cultivation studies indicate that the *Beta-* and *Gammaproteobacteria* are important metabolically active microbial groups to target during biostimulation experiments.
- LIBSHUFF and co-ancestry (data not shown) analysis indicated sequences obtained from the acidic pH sediments were more closely related to each other than sequences obtained from neutral pH sediments, suggesting a common selective pressure within these two sediment types. Interestingly, DNA- and RNA-derived clone sequences from similar sites were not closely related, highlighting variances in community compositions between these two clone targets.
- Building on these data collected from unstimulated sediments, we are currently characterizing the metabolically active fraction of the microbial community associated with the biostimulation of nitrate reduction and metal reduction in Area 1 sediment microcosms.

## ACKNOWLEDGMENTS

This research was funded by the Natural and Accelerated Bioremediation Research (NABIR) program, Biological and Environmental Research (BER) and U.S. Department of Energy (grant DE-FG02-00ER2986). I would like to thank Robert Arnold, Jon Delgado, David Swiford, Yangfeng Shi, Eric Jones, Dacia Drury, Steve Thompson, and Steve Miller for their support and collaboration on this project.